

Reaction of Phosphaalkynes with $[\text{Ru}_4(\text{CO})_{13}(\mu_3\text{-PPh})]$: Synthesis of Unsymmetrically Capped Bisphosphinidene Complexes[†]

Manfred Scheer,* Joachim Krug, Peter Kramkowski, and John F. Corrigan

Institut für Anorganische Chemie, Universität Karlsruhe, D-76128 Karlsruhe, Germany

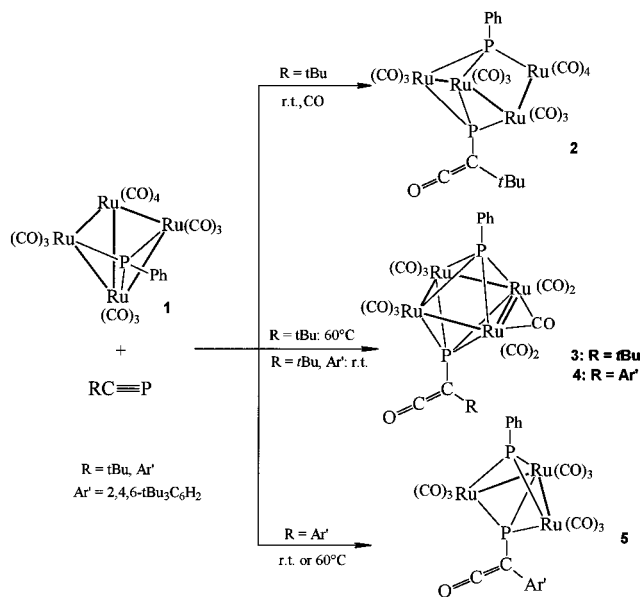
Received July 29, 1997[®]

The 62-electron cluster $[\text{Ru}_4(\text{CO})_{13}(\mu_3\text{-PPh})]$ (**1**) reacts with phosphalkynes $\text{RC}\equiv\text{P}$ [$\text{R} = \text{tBu}$, $\text{Ar}' (2,4,6\text{-tBu}_3\text{C}_6\text{H}_2)$] to yield a series of unsymmetrically capped bisphosphinidene clusters characterized by a ketene substituted $\mu_4\text{-PR}$ ligand. The reaction pathway was followed by ^{31}P -NMR spectroscopy and reveals that, in the first step of the reaction, a CO substitution of **1** occurs in order to form an intermediate with a σ - or π -bonded phosphalkyne. After scavenging of CO the chain compound $[\text{Ru}_4(\text{CO})_{12}(\mu_3\text{-PPh})(\mu_3\text{-PC}(\text{CO})\text{R})]$ [$\text{R} = \text{tBu}$ (**2**), Ar' (**7**)] is created. Further CO elimination leads to the *closo*-complexes $[\text{Ru}_4(\text{CO})_{10}(\mu\text{-CO})(\mu_4\text{-PPh})(\mu_4\text{-PC}(\text{CO})\text{R})]$ [$\text{R} = \text{tBu}$ (**3**), Ar' (**4**)]. Due to steric reasons the *nido*-cluster $[\text{Ru}_3(\text{CO})_9(\mu_3\text{-PPh})\{\mu_3\text{-PC}(\text{CO})\text{tBu}\}]$ (**5**) is the final product in the reaction starting from $\text{Ar}'\text{C}\equiv\text{P}$. The molecular structures of the complexes **2**–**5** are discussed.

Introduction

The detailed study of the reactivity of alkynes and related unsaturated organic molecules coordinated to metal cluster complexes continues to be the focus of many research efforts.¹ In this regard, the ability of flexible polymetallic frameworks to stabilize highly strained or reactive molecules via multiple-site coordination often enables full spectroscopic and structural characterization of the 'trapped' species. Recent examples of such strategies include the coordination of cyclobutadiene to a triosmium surface² and the trapping of phosphorus monoxide (PO) on a tetraruthenium cluster framework.³ The 62-electron *nido*- $[\text{Ru}_4(\text{CO})_{13}(\mu_3\text{-PPh})]$ (**1**) has been shown to possess a rich and diverse chemistry with alkynes and diynes. Examples of facile P–C bond formation, alkyne oligomerization, and skeletal transformations have been documented.⁴ Although the chemistry of phosphaalkynes ($\text{RC}\equiv\text{P}$) continues to develop at a rapid pace,⁵ details of the reactivity of these molecules on polymetallic surfaces are surprisingly scarce.⁶ The highly activated cluster

Scheme 1. Reaction of **1** with $\text{RC}\equiv\text{P}$



1 provides an opportunity to explore the chemistry of $\text{RC}\equiv\text{P}$ on cluster frames, and our findings are presented herein.

Results and Discussion

The reactions of $[\text{Ru}_4(\text{CO})_{13}(\mu_3\text{-PPh})]$ (**1**) with different phosphalkynes lead to various ketene ligand-containing clusters. The ligand $\text{tBuC}\equiv\text{P}$ reacts with **1** at ambient temperatures to yield the complex $[\text{Ru}_4(\text{CO})_{12}(\mu_3\text{-PPh})(\mu_3\text{-PC}(\text{CO})\text{tBu})]$ (**2**) (Scheme 1), whereas at 60°C the *closo*-complex $[\text{Ru}_4(\text{CO})_{10}(\mu\text{-CO})(\mu_4\text{-PPh})(\mu_4\text{-PC}(\text{CO})\text{tBu})]$ (**3**) is formed.

(b) Al-Resayes, S. I.; Hitchcock, P. B.; Nixon, J. F. *J. Chem. Soc., Chem. Commun.* **1987**, 929. (c) Gaede, P. E.; Johnson, B. F. G.; Nixon, J. F.; Nowotny, M.; Parsons, S. *J. Chem. Soc., Chem. Commun.* **1996**, 1455. (d) Bartsch, R.; Blake, A. J.; Johnson, B. F. G.; Jones, P. G.; Müller, C.; Nixon, J. F.; Nowotny, M.; Schmutzler, R.; Shephard, D. S. *Phosphorus, Sulfur, Silicon* **1996**, *115*, 201. (e) Byrne, L. T.; Johnson, J. A.; Koutsantonis, G. A.; Skelton, B. W.; White, A. H. *J. Chem. Soc., Chem. Commun.* **1997**, 391. (f) Lentz, D.; Michael H. *Angew. Chem.* **1989**, *101*, 330; *Angew. Chem., Int. Ed. Engl.* **1989**, *28*, 321.

[†] Dedicated to Professor W. Siebert on the occasion of his 60th birthday.

* Author to whom correspondence should be addressed. Fax: +49-(0)721661921. E-mail: mascheer@achim6.chemie.uni-karlsruhe.de.

[®] Abstract published in *Advance ACS Abstracts*, December 1, 1997.

(1) (a) Sappa, E. *J. Cluster Sci.* **1994**, *5*, 211. (b) Raithby, P. R.; Rosales, M. *J. Adv. Inorg. Chem. Radiochem.* **1985**, *29*, 169. (c) Sappa, E.; Tiripicchio, A.; Braunstein, P. *Chem. Rev.* **1983**, *83*, 203.

(2) (a) Adams, R. D.; Qu, X.; Wu, W. *Organometallics* **1994**, *13*, 1272. (b) Adams, R. D.; Qu, X.; Wu, W. *Organometallics* **1993**, *12*, 4117. (c) Adams, R. D.; Chen, G.; Qu, X.; Wu, W.; Yamamoto, J. H. *Organometallics* **1993**, *12*, 3029. (d) Adams, R. D.; Chen, G.; Qu, X.; Wu, W.; Yamamoto, J. H. *J. Am. Chem. Soc.* **1992**, *114*, 10977.

(3) (a) Wang, W.; Corrigan, J. F.; Doherty, S.; Enright, G.; Taylor, N. J.; Carty, A. J. *Organometallics* **1996**, *15*, 2770. (b) Corrigan, J. F.; Doherty, S.; Taylor, N. J.; Carty, A. J. *J. Am. Chem. Soc.* **1994**, *116*, 9799.

(4) (a) Corrigan, J. F.; Doherty, S.; Taylor, N. J.; Carty, A. J. *Organometallics* **1993**, *12*, 1365. (b) Corrigan, J. F.; Doherty, S.; Taylor, N. J.; Carty, A. J. *Organometallics* **1992**, *11*, 3160.

(5) Regitz, M.; Binger, P. *Angew. Chem.* **1988**, *100*, 1541; *Angew. Chem., Int. Ed. Engl.* **1988**, *27*, 1484. (b) Nixon, J. F. *Chem. Rev.* **1988**, *88*, 1327. (c) Binger, P. In *Multiple Bonds and Low Coordination in Phosphorus Chemistry*; Regitz, M., Scherer, O. J., Eds.; Thieme Verlag: Stuttgart, 1990. (d) Regitz, M. *Chem. Rev.* **1990**, *90*, 191. (e) Mack, A.; Regitz, M. *Chem. Ber.* **1997**, *130*, 823.

PC(CO)tBu] (**3**) is formed exclusively. Starting with the bulkier reagent Ar'C≡P (Ar' = 2,4,6-tBu₃C₆H₂) under either conditions the *closo*-complex [Ru₄(CO)₁₀(μ-CO)(μ₄-PPh)(μ₄-PC(CO)Ar')] (**4**) and the *nido*-cluster [Ru₃(CO)₉(μ₃-PPh)(μ₃-PC(CO)Ar')] (**5**) are obtained. A driving force for the formation of a ketene is clearly the generation of a flexible and strongly bound μ₃- or μ₄-phosphinidene ligand from the phosphalkyne and CO. The uptake of a CO molecule by the coordinatively unsaturated C atom of the methylidyne yields the ketene ligand. The formation of a ketene-substituted μ_n-phosphinidene ligand (*n* = 3, 4) was first observed in the complex [RePt(CO)₈(dppe){PC(=C=O)tBu}],^{6a} and more recently, additional examples were reported with the *closo*-clusters [Ru₃M{μ₄-PC(CO)tBu}₂(μ-CO)(CO)₁₀] (M = Ru, Fe)^{6b} and the *nido*-clusters [M₃{μ₃-PC(=C=O)tBu}₂(CO)₉] (M = Ru, Os)^{6c} and [Ru₃(μ-dppm)(CO)₇{μ₃-PC(CO)tBu}₂].^{6d}

The products **2–5** were separated and isolated by thick layer chromatography in fair yields. Complex **2** is a yellow, **3** a black, **4** a violet, and **5** a brown crystalline compound, all sparingly soluble in hexane but readily soluble in toluene and CH₂Cl₂. They were fully characterized on the basis of their spectroscopic data and by single-crystal X-ray analysis. In the IR spectra all compounds show the coupled vibration mode of the ketene group at ~2100 cm⁻¹. These values are comparable with those of organic ketenes of the type R₁R₂C=C=O.⁷ The CO stretching frequencies of terminal CO ligands in **2–5** are observed in the expected range of 2075–1980 cm⁻¹. For the *closo*-clusters **3** and **4** an additional vibration mode of the bridging CO ligand is found at 1817 cm⁻¹. In all cases the parent molecular ion peak was observed in the mass spectra, with the exception of **2**, where the highest fragment observed corresponds to a loss of Ru(CO)₄. ³¹P-NMR spectra revealed doublets for all products with a small J_{PP} coupling constant for the *closo*-complexes **3** (89 Hz) and **4** (73 Hz) and larger coupling constants (179 Hz) for the unsaturated complexes **2** and **5**.

X-ray analyses of all products provided full structural details. The molecular structure of **2** (Figure 1) reveals that the molecular frame "opens" to yield four Ru atoms in an open and bent chain. The PPh and PC(=C=O)tBu groups are μ₃-capping, but to different Ru atoms. Cluster **2** is produced in low yield (11%) from the reaction of **1** with tBuC≡P, presumably scavenging its fourteenth carbonyl ligand from CO molecules substituted on **1** (*vide infra*). Attempts to increase the yield via a CO purge into the reaction mixture resulted instead in no reaction between **1** and the phosphalkyne taking place. The structure of the Ru₄P₂ core cannot be described in terms of a parent deltahedron, unlike in **3** and **4** (*n*+1 skeletal pairs, *closo*-octahedron) and **5** (*n*+2, *nido*-Ru₃P₂ octahedron; Figure 2). The two phosphinidene ligands in **2** cap opposite sides of the open Ru₄ frame [Ru(1)–P(1) = 2.408(1), Ru(2)–P(1) = 2.330(1), Ru(4)–P(1) = 2.352(2), Ru(1)–P(2) = 2.382(1), Ru(2)–P(2) = 2.380(2), Ru(3)–P(2) = 2.426(1) Å] sharing two common vertices [Ru(1) and Ru(2)]. It is noteworthy that the ³¹P chemical shift for μ₃-PPh in **2** is at

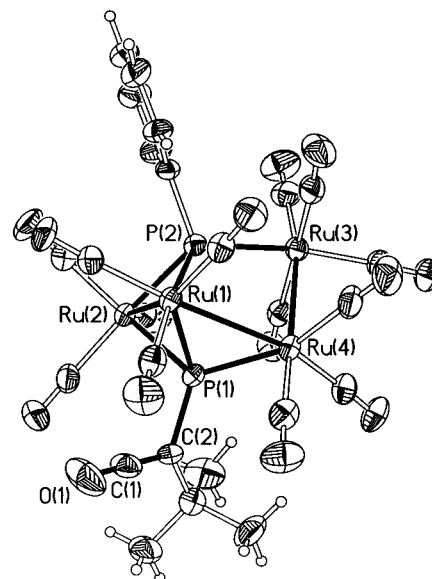


Figure 1. Molecular structure of [Ru₄(CO)₁₃(μ₃-PPh){μ₃-PC(CO)tBu}] (**2**) (ellipsoids drawn at 50% probability level). Selected bond distances (Å) and angles (deg): Ru(1)–Ru(2) 2.9073(10), Ru(1)–Ru(4) 2.9300(8), Ru(3)–Ru(4) 2.9118(12), Ru(1)–P(1) 2.4076(13), Ru(1)–P(2) 2.3828(14), Ru(2)–P(1) 2.3296(14), Ru(2)–P(2) 2.380(2), Ru(4)–P(1) 2.352(2), Ru(3)–P(2) 2.4264(13), P(1)–C(2) 1.836(3), P(2)–C(7) 1.849(5), C(1)–O(1) 1.166(7), C(1)–C(2) 1.302(7), C(2)–C(3) 1.535(8), O(1)–C(1)–C(2) 179.2(8), Ru(2)–Ru(1)–Ru(4) 91.73(3), Ru(3)–Ru(4)–Ru(1) 102.9(2), C(1)–C(2)–C(3) 121.4(5).

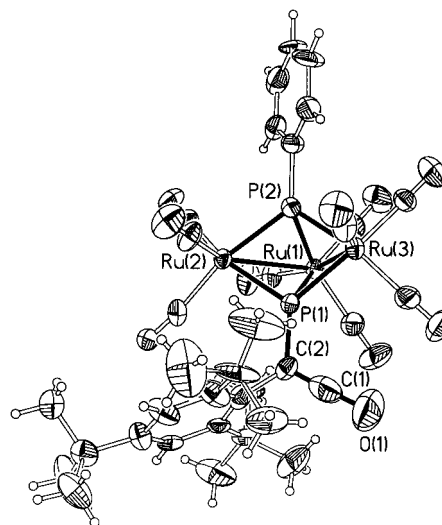


Figure 2. Molecular structure of [Ru₃(CO)₉(μ₃-PPh){μ₃-PC(CO)Ar'}] (**5**) (ellipsoids drawn at 50% probability level). Selected bond distances (Å) and angles (deg): Ru(1)–Ru(2) 2.906(2), Ru(1)–Ru(3) 2.8641(14), Ru(1)–P(1) 2.419(2), Ru(1)–P(2) 2.353(3), Ru(2)–P(1) 2.338(3), Ru(2)–P(2) 2.359(3), Ru(3)–P(1) 2.352(3), Ru(3)–P(2) 2.334(3), P(1)–C(2) 1.807(13), P(2)–C(21) 1.815(13), C(1)–O(1) 1.27(3), C(1)–C(2) 1.21(3), C(2)–C(3) 1.47(2), O(1)–C(1)–C(2) 176(2), Ru(3)–Ru(1)–Ru(2) 82.53(4), C(1)–C(2)–C(3) 117.0(14).

approximately 165 ppm higher field versus that of **1**.⁸ Whereas in **1** the phosphinidene ligand caps a Ru₃ triangle of metal atoms with one nonbonded Ru...Ru contact, in **2** the triangle defined by Ru(1)–Ru(2)–Ru(3) has one metal–metal bond. The second phosphinidene unit, arising from the attack of CO on tBuC≡P, caps a

(7) Schaumann, E.; Scheiblich, S. *Houben-Weyl, Methoden der Organischen Chemie*, 4th ed.; Thieme Verlag: Stuttgart, 1990; Vol. E15/2.

(8) Cherkas, A. A.; Corrigan, J. F.; Doherty, S.; MacLaughlin, S. A.; Van Gastel, F.; Taylor, N. J.; Carty, A. J. *Inorg. Chem.* **1993**, *32*, 1662.

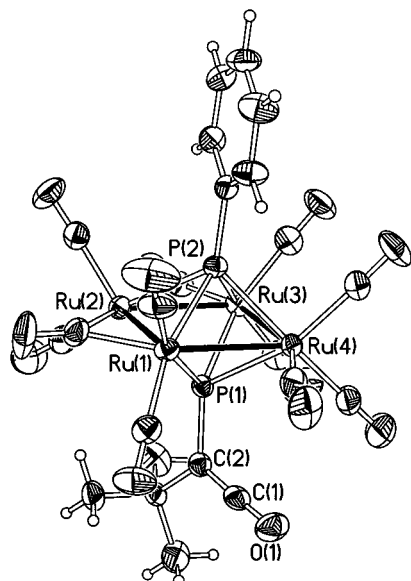


Figure 3. Molecular structure of $[Ru_4(\mu\text{-CO})(CO)_{10}(\mu_4\text{-PPh})\{\mu_4\text{-PC(CO)tBu}\}]$ (**3**) (ellipsoids drawn at of 50% probability level). Selected bond distances (Å) and angles (deg): Ru(1)–Ru(2) 2.7031(8), Ru(1)–Ru(4) 2.8687(13), Ru(2)–Ru(3) 2.9089(13), Ru(3)–Ru(4) 2.8613(8), Ru(1)–P(1) 2.4757(13), Ru(1)–P(2) 2.4728(14), Ru(2)–P(1) 2.5279(13), Ru(2)–P(2) 2.3815(12), Ru(4)–P(1) 2.3999(13), Ru(3)–P(1) 2.4069(13), Ru(3)–P(2) 2.3902(12), Ru(4)–P(2) 2.3815(12), P(1)–C(2) 1.796(4), P(2)–C(7) 1.803(4), C(1)–O(1) 1.160(7), C(1)–C(2) 1.314(6), C(2)–C(3) 1.535(5), O(1)–C(1)–C(2) 178.1(8), Ru(1)–Ru(2)–Ru(3) 90.86(3), Ru(2)–Ru(1)–Ru(4) 91.73(3), Ru(3)–Ru(4)–Ru(1) 88.56(3), Ru(4)–Ru(3)–Ru(2) 88.29(3), C(1)–C(2)–C(3) 120.9(4), P(1)–C(2)–C(3) 127.1(3).

Ru_3 fragment with one open edge. The ^{31}P shift associated with this phosphorus atom ($\delta = 149$ ppm) lies in the range of those observed in related, 'open' $[Ru_3\{\mu_3\text{-PC(=C=O)tBu}\}_2]$ clusters.^{6c,d} There is little difference observed between the Ru–P bonding distances of the two ligands.

The X-ray structures of **3** (Figure 3) and **4** (Figure 4) reveal a square-planar Ru_4 core each μ_4 -capped by the two different phosphinidene ligands, PPh and PC(=C=O)R, respectively, to form distorted octahedra. These octahedra are electron precise within the formalism of polyhedral skeletal electron pair theory (7 pairs, 6 vertices) but electron deficient according to the effective atomic number rule (62 electrons, 4 metal atoms with 4 M–M bonds). This unsaturation manifests itself in the NMR parameters observed in both **3** and **4**. The high-field shifts in the ^{31}P -NMR spectra (**3** = 119, 196; **4** = 169, 196 ppm) contrast with those observed for electron precise (64 electron) $M_4(\mu_4\text{-PR})$ species.⁹ Recent solid-state CP/MAS ^{31}P -NMR experiments by Wasylshen and co-workers on related unsaturated complexes rule out any ring current effects arising from the unsaturated M_4 core as being responsible for the observed high-field shifts.¹⁰

For **4** two independent molecules with essentially identical bonding parameters were found. In further

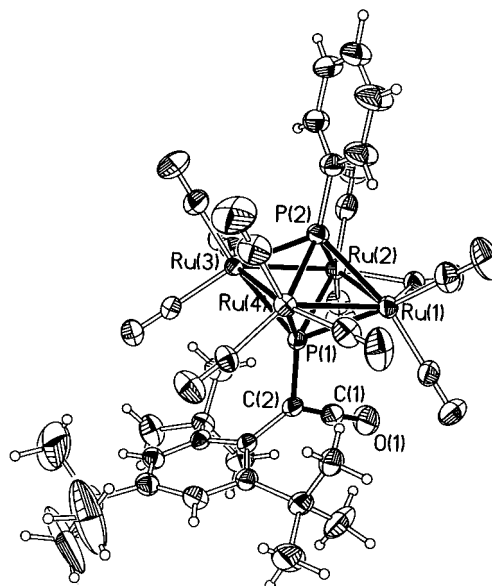


Figure 4. Molecular structure of $[Ru_4(\mu\text{-CO})(CO)_{10}(\mu_4\text{-PPh})\{\mu_4\text{-PC(CO)Ar'}\}]$ (**4**) (molecule A) (ellipsoids drawn at 50% probability level). Selected bond distances (Å) and angles (deg): Ru(1)–Ru(2) 2.712(1), Ru(1)–Ru(4) 2.901(1), Ru(2)–Ru(3) 2.866(1), Ru(3)–Ru(4) 2.851(1), Ru(1)–P(1) 2.477(1), Ru(1)–P(2) 2.477(1), Ru(2)–P(1) 2.512(1), Ru(2)–P(2) 2.455(1), Ru(4)–P(1) 2.391(1), Ru(3)–P(1) 2.425(1), Ru(3)–P(2) 2.390(1), Ru(4)–P(2) 2.383(1), P(1)–C(2) 1.825(4), P(2)–C(7) 1.803(4), C(1)–O(1) 1.146(7), C(1)–C(2) 1.314(6), C(2)–C(3) 1.495(6), O(1)–C(1)–C(2) 178.1(6), Ru(1)–Ru(2)–Ru(3) 91.96(2), Ru(2)–Ru(1)–Ru(4) 90.82(2), Ru(3)–Ru(4)–Ru(1) 88.46(2), Ru(4)–Ru(3)–Ru(2) 88.76(2), C(1)–C(2)–C(3) 127.7(4), P(1)–C(2)–C(3) 122.8(3).

discussions only molecule A is described. The Ru(1)–Ru(2) distances in **3** and **4** [2.703(1) and 2.712(1) Å, respectively] are significantly shorter than the other metal–metal bonds [2.851(1)–2.909(1) Å] and can be formally regarded as double bonds. The structural features are analogous to those of the tetranuclear clusters of $[M_4(\mu_4\text{-PPh})_2(\mu\text{-CO})(CO)_{10}]$ (M = Ru, Fe), $[Co_2Fe_2(\mu_4\text{-PPh})_2(\mu\text{-CO})(CO)_{10}]$,¹¹ and, more recently, $[Ru_4\{\mu_4\text{-PC(=C=O)tBu}\}_2(\mu\text{-CO})(CO)_{10}]$.^{6b} Clusters **3** and **4** represent the first examples of unsymmetrically capped M_4PP' complexes containing a ketene-substituted phosphinidene ligand. Recent efforts have led to the isolation and structural characterization of mixed group 15/16 bicapped Ru_4 and Fe_4 clusters,¹² and work by Mathur and co-workers has also led to the generation of a variety of mixed metal-mixed chalcogenide (Fe/Ru/Se/Te) M_4E_2 complexes.¹³ The ketene groups in **3** and **4** are orientated in different ways, reflecting the different steric influence of the substituents tBu and Ar'. While in the tBu derivative **4** it is directed towards atom

(11) (a) Jaeger, J. T.; Field, J. S.; Collison, D.; Speck, G. P.; Peake, D. M.; Hähnle, J.; Vahrenkamp, H. *Organometallics* **1988**, *7*, 1753. (b) Vahrenkamp, H.; Wolters, D. *J. Organomet. Chem.* **1982**, *224*, C17. (c) Vahrenkamp, H.; Wucherer, E. J.; Wolters, D. *Chem. Ber.* **1983**, *116*, 1219. (d) Jaeger, J. T.; Aime, S.; Vahrenkamp, H. *Organometallics* **1986**, *5*, 245. (e) Field, J. S.; Haines, R. J.; Smit, D. N.; Natarajan, K.; Scheidsteger, O.; Huttner, G. *J. Organomet. Chem.* **1986**, *240*, C23. (f) Field, J. S.; Haines, R. J.; Smit, D. N. *J. Chem. Soc., Dalton Trans.* **1988**, 1315.

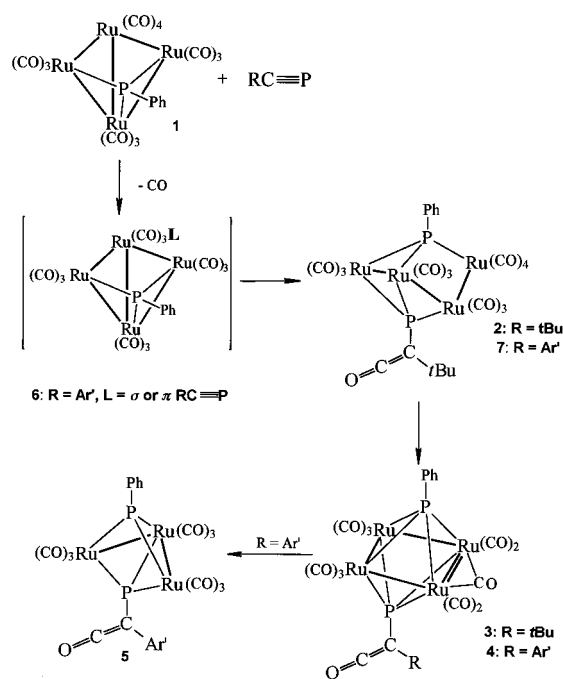
(12) (a) Van Gastel, F.; Agocs, L.; Cherkas, A. A.; Corrigan, J. F.; Doherty, S.; Ramachandran, R.; Taylor, N. J.; Carty, A. J. *J. Cluster Sci.* **1991**, *2*, 131. (b) Eber, B.; Buchholz, D.; Huttner, G.; Fassler, Th.; Imhof, W.; Fritz, M.; Joachims, J. C.; Daran, J. C.; Jeannin, Y. *J. Organomet. Chem.* **1991**, *401*, 49.

(13) Mathur, P.; Chakrabarty, D.; Hossain, Md. M. *J. Organomet. Chem.* **1991**, *418*, 415.

(9) (a) Knox, S. A. R.; Lloyd, B. R.; Orpen, A. G.; Vinas, J. M.; Weber, M. J. *Chem. Soc., Chem. Commun.* **1987**, 1498. (b) Corrigan, J. F.; Doherty, S.; Taylor, N. J.; Carty, A. J. *J. Chem. Soc., Chem. Commun.* **1991**, 1640.

(10) Eichele, K.; Wasylshen, R. E.; Corrigan, J. F.; Taylor, N. J.; Carty, A. J. *J. Am. Chem. Soc.* **1995**, *117*, 6961.

Scheme 2. Proposed Reaction Pathway of 1 with RC≡P



Ru(4), the $\text{PC}(\text{C}=\text{O})\text{Ar}'$ unit in **4** is orientated toward the bridging CO ligand. The angle $\text{P}(1)\text{-C}(2)\text{-C}(3)$ is less bent in **4** [122.8(3)] than in the tBu derivative **3** [127.1(3)]. The average Ru–P bond lengths of the ketene phosphinidene in both **3** and **4** are markedly longer than the phenylphosphinidene ligand capping the opposite side of the Ru_4 square face [**3** Ru–P(1) = 2.453(2), Ru–P(2) = 2.407(2); **4** Ru–P(1) = 2.451(2), Ru–P(2) = 2.426(2) Å av]. The bonding parameters of the ketene groups in **2–5** are comparable with those of known organic ketenes and the aforementioned phospho-substituted ketenes. The P(1)–C(2) bond lengths of the $\text{PC}(\text{CO})\text{R}$ unit are 1.836(3) Å in **2**, 1.807(13) Å in **5**, 1.795(4) Å in **3**, and 1.825(4) Å in **4** compared with 1.548(1)^{14a} and 1.516(13)^{14b} Å in the free phosphalkynes (tBuC≡P and Ar'C≡P), respectively, and correspond to the single-bond nature of the P–C bond.

Studies of the Reaction Pathway. In an attempt to gain insight into the reaction pathway, the reactions of $[\text{Ru}_4(\text{CO})_{13}(\mu_3\text{-PPh})]$ (**1**) with Ar'C≡P and tBuC≡P, respectively, were followed by ³¹P-NMR spectroscopy. In the reaction with tBuCP at ambient temperature only the signals for the starting material **1**, free phosphalkyne, and the end product **2** were observed. Increasing the reaction temperature to 60 °C resulted in a marked and rapid decrease in the amount of **2** in favor of an increase of the unsaturated complex **3**. No intermediate was detectable (Scheme 2).

The reaction of **1** with Ar'C≡P is much slower and does not proceed at room temperature. At 40 °C, however, it is possible to follow the reaction over time. In addition to signals of the starting materials $[\text{Ru}_4(\text{CO})_{13}(\mu_3\text{-PPh})]$ (**1**) ($\delta = 407.9$ ppm) and Ar'C≡P ($\delta = 34.4$ ppm), two singlets at 397.2 and 30.7 ppm were observed after 30 min representing, presumably, the

first intermediate along the reaction pathway. These signals can be tentatively assigned to a complex of the formula $[\text{Ru}_4(\text{CO})_{12}(\mu_3\text{-PPh})(\text{P}\equiv\text{CAR}')]$ (**6**) with either a σ - or π -bonded phosphalkyne formed after CO substitution. The loss of CO during this first step of coordination may be the source of the ketene units present in products **2–5**. The attack of the phosphalkyne can proceed via an end-on coordination or, more probably, via a side-on ligating mode. The possibility of σ -coordination of the phosphalkyne in **6** is, however, supported by reaction of **1** with PPhMe₂. This results in the formation of the complex $[\text{Ru}_4(\text{CO})_{12}(\mu_3\text{-PPh})(\text{PPhMe}_2)]$, where CO substitution occurs on the unique hinge Ru atom with four carbonyl ligands in **1** and whose NMR data ($\delta = 406.6$ (s) and 0.11 (s) ppm) closely resemble that observed in **6**.¹⁵ Related chemistry of **1** with alkynes shows a strong tendency for σ, σ, π -coordination of unsaturated organics on the Ru_3P square face. In **1**, however, such complexes display a diagnostic high-field shift in the ³¹P-NMR spectrum due to the five coordinate nature of the phosphorus atom.¹⁶ The coordination of phosphalkynes in such a manner was proposed as an intermediate en route to ketenyl phosphinidene ligands on Ru_3 clusters^{6d} and would parallel the chemistry of nitriles on polymetallic surfaces.¹⁷

After 1 h of further heating, two additional doublets at 222.0 and 267.0 ppm ($J_{\text{PP}} = 141$ Hz) are observed, which lie in the range of those found in the isolated complex $[\text{Ru}_4(\text{CO})_{13}(\mu_3\text{-PPh})\{\mu_3\text{-PC}(\text{CO})\text{tBu}\}]$ (**2**) ($\delta = 158$ (d), 246 (d) and $J_{\text{PP}} = 179$ Hz). The related Ar'-substituted complex $[\text{Ru}_4(\text{CO})_{13}(\mu_3\text{-PPh})\{\mu_3\text{-PC}(\text{CO})\text{Ar}'\}]$ (**7**) can thus be suggested. Concomitant with the appearance of these signals, those assigned to the *closo*-complex **4** began to appear. After an additional hour the signals for the initial compound **6** decreased in intensity, and those assigned to **7** disappeared, whereas the amount of **4** increased, and the doublets assigned to the trinuclear complex *nido*-**5** also appeared. The intensity of the signals for **4** and **5** increased over a total period of 3 h; however, after 6 h the *closo*-cluster **4** was no longer observed with **5** representing the only product present. Cluster **4** is obviously transformed to **5** by the elimination of $\text{Ru}(\text{CO})_2$, which can be experimentally verified: heating a solution of **4** in benzene for 6 h at 60 °C results in the formation of **5** as the only phosphorus-containing species detectable by NMR. In the related reaction of **1** with tBuC≡P even with longer reaction times and elevated temperatures there was no evidence for the formation of a related *nido*-cluster $[\text{Ru}_3(\text{CO})_9(\mu_3\text{-PPh})\{\mu_3\text{-PC}(\text{C}=\text{O})\text{tBu}\}]$ as the final product. Obviously, the steric influence of the supermesityl group in **4** results in a greater stability of the trinuclear complex *nido*-**5** versus *closo*-**4**.

These results support the reaction pathway shown in scheme 2: $[\text{Ru}_4(\text{CO})_{13}(\mu_3\text{-PPh})]$ (**1**) reacts with $\text{RC}\equiv\text{P}$ to give $[\text{Ru}_4(\text{CO})_{12}(\mu_3\text{-PPh})(\text{PCAR}')]$ (**6**) as the first formed product monitored starting with Ar'C≡P. The next step of the reaction seems to be the scavenging of CO to give the chain compounds $[\text{Ru}_4(\text{CO})_{13}(\mu_3\text{-PPh})\{\mu_3\text{-PC}(\text{CO})\text{-Ar}'\}]$ (**2**) (R = tBu) and **7** (R = Ar'). Further heating is accompanied by CO elimination to yield the *closo*-

(14) (a) Chernega, A. N.; Antipin, M. Y.; Struchkov, T.; Meidine, M. F.; Nixon, J. F. *Heteroatom Chem.* **1991**, *2*, 665. (b) Arif, A. M.; Barron, A. R.; Cowley, A. H.; Hall, S. W. *J. Chem. Soc., Chem. Commun.* **1988**, 171.

(15) Van Gastel, Ph.D. Dissertation, University of Waterloo, 1991.
(16) Corrigan, J. F.; Doherty, S.; Taylor, N. J.; Carty, A. J. *J. Am. Chem. Soc.* **1992**, *114*, 7557.

(17) Suter, P.; Vahrenkamp, H. *Chem. Ber.* **1995**, *128*, 793.

Table 1. Crystallographic Data for 2–5

	2·0.5C ₆ H ₆	3	4	5
formula	C ₂₈ H ₂₀ O ₁₄ P ₂ Ru ₄	C ₂₃ H ₁₄ O ₁₂ P ₂ Ru ₄	C ₃₇ H ₃₄ O ₁₂ P ₂ Ru ₄	C ₃₅ H ₃₄ O ₁₀ P ₂ Ru ₃
formula wt	1043.64	948.56	1136.86	979.76
cryst size, mm	0.27 × 0.21 × 0.08	0.3 × 0.18 × 0.07	0.27 × 0.21 × 0.08	0.11 × 0.08 × 0.04
T, K	200(1)	200(1)	200(1)	200(1)
space group	$P\bar{1}$ (No. 2)	$P\bar{1}$ (No. 2)	$P2_1/n$ (No. 14)	$P\bar{1}$ (No. 2)
cryst syst	triclinic	triclinic	monoclinic	triclinic
a, Å	10.078(2)	9.448(2)	12.040(2)	9.620(2)
b, Å	10.393(2)	10.078(3)	42.290(9)	13.340(3)
c, Å	18.108(4)	17.343(6)	16.480(3)	15.440(3)
α, deg	105.63(3)	105.26(3)	90	86.96(3)
β, deg	106.48(3)	91.70(2)	91.61(3)	82.82(3)
γ, deg	90.02(3)	108.70(2)	90	84.62(3)
V, Å ³	1745.4(6)	1497.2(8)	8388(3)	1955.5(7)
Z	2	2	8	2
d _c , g/cm ³	1.986	2.104	1.801	1.61
μ _c , cm ⁻¹	18.53	21.43	15.47	12.77
radiation (λ, Å)			Mo Kα (0.71073)	
diffractometer	STOE IPDS	STOE STADI IV	STOE IPDS	STOE IPDS
2θ range, deg	6.12 ≤ 2θ ≤ 54.1	4.42 ≤ 2θ ≤ 52	5.04 ≤ 2θ ≤ 52.1	4 ≤ 2θ ≤ 55.8
hkl range	-12 ≤ h, k ≤ 12, -21 ≤ l ≤ 23	-11 ≤ h ≤ 9, -12 ≤ k ≤ 11, 0 ≤ l ≤ 21	-13 ≤ h ≤ 13, -35 ≤ k ≤ 51, -19 ≤ l ≤ 20	-12 ≤ h ≤ 12, -17 ≤ k ≤ 17, -20 ≤ l ≤ 17
data/restraints/parameters	6338/0/436	5684/0/373	12449/0/1009	7849/0/451
independent reflections with I > 2σ(I)	5488 (R _{int} = 0.0234)	4248 (R _{int} = 0.0000)	11553 (R _{int} = 0.0341)	3636 (R _{int} = 0.0921)
goodness-of-fit on F ²	1.104	0.998	1.088	1.001
R ₁ , ^a wR ₂ ^b (I > 2σ(I))	0.0345, 0.0950	0.0253, 0.0530	0.0342, 0.0922	0.0694, 0.1151
R ₁ , ^a wR ₂ ^b (all data)	0.0419, 0.1128	0.0471, 0.0642	0.0375, 0.0988	0.1804, 0.1564
weight factors a, b ^c	0.0637, 4.3108	0.0250, 0	0.0487, 14.6014	0.0460, 0
largest diff peak, hole, e/Å ³	0.751, -1.131	0.602, -0.498	0.884, -0.577	1.111, -0.684

^a $R = \sum |F_0| - |F_c| / \sum |F_0|$. ^b $wR_2 = [\sum \omega(F_0^2 - F_c^2)^2] / [\sum (F_0^2)^2]^{1/2}$. ^c $\omega^{-1} = \sigma^2(F_0^2) + aP^2 + bP$; $P = [F_0^2 + 2F_c^2]/3$.

clusters $[Ru_4(\mu\text{-CO})(CO)_{10}(\mu_4\text{-PPh})\{\mu_4\text{-PC}(\text{CO})\text{R}\}]$ (**3** and **4**). This skeletal rearrangement process would parallel observations for the related molecule $[Ru_4(CO)_{11}(\mu_4\text{-PPh})_2]$ which reversibly uptakes CO, accompanied by an opening of the metal framework.^{11e} Cluster **3** is the final product of the reaction starting with $t\text{BuC}\equiv\text{P}$, whereas the *nido*-cluster $[Ru_3(CO)_9(\mu_3\text{-PPh})\{\mu_3\text{-PC}(\text{CO})\text{-Ar}\}]$ (**5**) is ultimately formed when the bulkier phosphaalkyne $\text{Ar}'\text{C}\equiv\text{P}$ is used.

Experimental Section

All experiments were performed under argon in anhydrous solvents. NMR: Bruker AC 250 (¹H, 250.13 MHz; ³¹P, 101.256 MHz); standard Me₄Si (¹H), 85% H₃PO₄ (³¹P). MS: Finnigan MAT 311 ADF at 70 eV. IR: Perkin-Elmer PE 883. Thick layer chromatography was performed on Merck silicagel plates.

Materials. Unless otherwise stated, commercial-grade chemicals were used without further purification. $[Ru_4(CO)_{13}(\mu_3\text{-PPh})]$ (**1**) was prepared in a modification of the procedure described in ref 8. $t\text{BuC}\equiv\text{P}$ was synthesized as described in ref 18, and $\text{Ar}'\text{C}\equiv\text{P}$ was prepared in a modified procedure as published in ref 19.

Crystal Structure Analysis of 2–5. Crystal structure analyses were performed on STOE IPDS (**2**, **4**, and **5**) and STOE STADI IV (**3**: ω-scan mode) diffractometers with Mo Kα radiation (λ = 0.710 73 Å) with empirical absorption corrections for **3** (five psi-scans). Machine parameters, crystal data, and data collection parameters are summarized in Table 1. The structures were solved by direct methods using SHELXS-86,^{20a} a full-matrix least-squares refinement on F² in SHELXL-93^{20b} with anisotropic displacement for non-H

atoms, hydrogen atoms located in idealized positions and refined isotropically according to the riding model.

[Ru₄(CO)₁₃(μ₃-PPh){μ₃-PC(CO)tBu}] (**2**). To 24 mg (0.027 mmol) of $[Ru_4(CO)_{13}(\mu_3\text{-PPh})]$ (**1**) in 5 mL of toluene was added 0.027 mmol of $t\text{BuC}\equiv\text{P}$ of a 0.5 M solution in *n*-hexane at ambient temperature. The reaction was monitored by ³¹P-NMR spectroscopy and was worked up on thick layer chromatography plates (CH₂Cl₂/hexane, 1:5) when the doublets assigned to **2** were detected (about 4 h). The yellow fraction was separated and extracted with CH₂Cl₂ and the solvent removed *in vacuo*. The residue was dissolved in *n*-hexane. Yellow crystals of **2** crystallized at 8 °C (9 mg, 11%). Crystals suitable for X-ray analysis were grown from concentrated benzene solutions. Anal. Calcd (found) for C₂₅H₁₄O₁₄P₂Ru₄: C, 29.77 (28.53); H, 1.40 (1.17). IR (*n*-hexane, cm⁻¹): ν = 2100(m), 2062(s), 2041(s), 2017(m), 1997(m). ¹H NMR (250.13 MHz, 25 °C, C₆D₆): δ 1.06 (s, 9H, tBu), 7.1 (m, 5H, Ph). ³¹P NMR (101.26 MHz, 25 °C, C₆D₆): δ 158 (d, P(1)), 246 (d, P(2)), J(P,P) = 179 Hz. EI MS: *m/z* (%) = 791.5 (3.6) [M - Ru(CO)₄]⁺, 763.6 (5.8) [M - Ru(CO)₅]⁺, 708.6 (6.9) [M - Ru(CO)₇]⁺, 680.5 (14.2) [M - Ru(CO)₈]⁺, 651.7 (14.4) [M - Ru(CO)₉]⁺.

[Ru₄(μ-CO)(CO)₁₀(μ₄-PPh){μ₄-PC(CO)tBu}] (**3**). To 24 mg (0.027 mmol) of **1** in 10 mL of *n*-hexane was added 0.027 mmol of $t\text{BuC}\equiv\text{P}$ of a 0.5 M *n*-hexane solution at ambient temperature. The reaction mixture was stirred for 4 h at 60 °C accompanied by a color change from light to dark red. The reaction was monitored by IR spectroscopy (carbonyl region) and thin layer chromatography. The reaction was stopped and worked up by thick layer chromatography (CH₂-Cl₂/hexane, 1:3) when no traces of **1** were observed. The dark brown fraction was separated and extracted with CH₂Cl₂, the solvent removed in vacuum, and the residue taken up in *n*-hexane to afford, at 2 °C, 14 mg (55%) of black crystals of **3**. Anal. Calcd (found) for C₂₃H₁₄O₁₂P₂Ru₄: C, 29.00 (28.81); H, 1.48 (1.27). IR (*n*-hexane, cm⁻¹): ν = 2101(m), 2075(m), 2035(s), 2018(s), 1980(s), 1817(m). ¹H NMR (250.13 MHz, 25 °C, C₆D₆): δ = 1.01 (s, 9H, tBu), 7.1 (m, 5H, Ph). ³¹P NMR (101.26 MHz, 25 °C, C₆D₆): δ = 119 (d, P(1)), 196 (d, P(2)), J(P,P) = 89 Hz. EI MS: *m/z* (%) = 951 (3.0) [M]⁺, 923 (2.4)

(18) Rösch, W.; Alspach, T.; Bergsträsser, U.; Regitz, M. In *Synthetic Methods of Organometallic and Inorganic Chemistry*; Herrmann, W. A.; Ed.; G. Thieme Verlag: Stuttgart, 1996; pp 13.

(19) Märkl, G.; Sejpká, H. *Tetrahedron Lett.* **1986**, *27*, 171. Sejpká, H. Ph.D. Thesis, University of Regensburg, 1987.

(20) (a) Sheldrick, G. M. SHELXS-86; University of Göttingen, 1986. (b) Sheldrick, G. M. SHELXL-93; University of Göttingen, 1993.

[M-(CO)]⁺, 895 (0.4) [M-2(CO)]⁺, 867 (2.2) [M-3(CO)]⁺, 839 (2.0) [M-4(CO)]⁺, 811 (3.4) [M-5(CO)]⁺, 783(4.4) [M-6(CO)]⁺, 755 (3.6) [M-7(CO)]⁺, 727 (2.8) [M-8(CO)]⁺, 699 (3.0) [M-9(CO)]⁺, 671 (2.8) [M-10(CO)]⁺, 643 (3.2) [M-11(CO)]⁺.

[Ru₄(μ-CO)(CO)₁₀(μ₄-PPh){μ₄-PC(CO)Ar'}] (4). Ar'C≡P (5.2 mg, 0.018 mmol) was added to 16 mg (0.018 mmol) of **1** in 10 mL of *n*-hexane at ambient temperature. The mixture was heated for 2 h at 45 °C. Workup on TLC plates gave a dark red fraction (CH₂Cl₂/hexane, 1:5) which was extracted with CH₂Cl₂ and recrystallized from *n*-hexane at 2 °C. Yield: 11 mg (35%) of dark red crystals of **4**. Anal. Calcd (found) for C₃₇H₃₂O₁₂P₂Ru₄: C, 39.02 (38.93); H, 2.83 (2.57). IR (*n*-hexane, cm⁻¹): ν = 2102(s), 2079(s), 2048(sh), 2038(s), 2021(s), 1982(s), 1817(m). ¹H NMR (250.13 MHz, 25 °C, C₆D₆): δ 1.19 (s, 9H, tBu), 1.23 (s, 18H, tBu), 7.1 (m, 5H, Ph), 7.21 (s, 2H, Ar'). ³¹P NMR (101.26 MHz, 25 °C, C₆D₆): δ 169 (d, P(1)), 196 (d, P(2)), *J*(P,P) = 73 Hz. EI MS: *m/z* (%) = 1139 (4.5) [M]⁺, 1111 (4.7) [M (CO)]⁺, 1083 (1.5) [M-2(CO)]⁺, 1055 (4.6) [M-3(CO)]⁺, 1027 (4.8) [M-4(CO)]⁺, 999 (16) [M-5(CO)]⁺, 971 (6.4) [M-6(CO)]⁺, 943 (6.5) [M-7(CO)]⁺, 915 (8) [M-8(CO)]⁺, 887 (8.1) [M-9(CO)]⁺, 859 (7.5) [M-10(CO)]⁺, 831 (8) [M-11(CO)]⁺.

[Ru₃(CO)₉(μ₃-PPh){μ₃-PC(CO)Ar'}] (5). To 24 mg (0.027 mmol) of **1** in 10 mL of *n*-hexane was added 7.8 mg (0.027 mmol) Ar'C≡P at ambient temperature. The mixture was stirred for 8 h at 60 °C accompanied by a color change from light red to brown. ³¹P-NMR identified **5** as the only phosphorus-containing product. Work up on thick layer chromatography plates gave a yellow fraction (CH₂Cl₂/hexane, 1:3)

which was separated and extracted with CH₂Cl₂. The solvent was removed and the residue dissolved in *n*-hexane; 16 mg (65%) of **5** crystallized at 8 °C. Anal. Calcd (found) for C₃₅H₃₂O₁₀P₂Ru₃: C, 42.86 (42.20); H, 3.29 (3.08). IR (*n*-hexane, cm⁻¹): ν = 2102(s), 2077(s), 2061(w), 2045(sh), 2037(s), 2021(m), 1984(w). ¹H NMR (250.13 MHz, 25 °C, C₆D₆): δ 1.25 (s, 9H, tBu), 1.36 (s, 18H, tBu), 7.2 (m, 5H, Ph), 7.42 (s, 2H, Ar'). ³¹P NMR (101.26 MHz, 25 °C, C₆D₆): δ = 217 (d, P(1)), 225 (d, P(2)), *J*(P,P) = 179 Hz. EI MS: *m/z* (%) = 979 (4.1) [M]⁺, 951 (4.3) [M-(CO)]⁺, 923 (3.8) [M-2(CO)]⁺, 895 (0.5) [M-3(CO)]⁺, 867 (4.7) [M-4(CO)]⁺, 839 (2.6) [M-5(CO)]⁺, 811 (3.7) [M-6(CO)]⁺, 783 (3.7) [M-7(CO)]⁺, 755 (3.8) [M-8(CO)]⁺, 727 (4.0) [M-9(CO)]⁺.

Acknowledgment. We are grateful to the *Deutsche Forschungsgemeinschaft* and the *Fonds der Chemischen Industrie* for comprehensive financial support of our work. The authors thank *Degussa AG* for the gift of RuCl₃·H₂O.

Supporting Information Available: Tables of crystal data, fractional coordinates, anisotropic displacement parameters, and bond lengths and angles and fully labeled figures showing 30% thermal ellipsoids and hydrogen atom coordinates for **2–5** (41 pages). Ordering information is given on any current masthead page.

OM970649L